International Journal of Concrete Structures and Materials

RESEARCH

Open Access

Optimized Machine Learning Algorithms for Predicting the Punching Shear Resistance of Flat Slabs with Transverse Reinforcement

Hua-Jun Yan[1*] and Nan Xie[1]

Abstract

In the calculation of reinforced concrete (RC) flat slabs with transverse reinforcement, punching shear resistance is one of the most critical factors. It is true that design provisions may be implemented, but they often result in significant biases and deviations from expectations. This study aims to present an optimized machine learning (ML) algorithm for estimating the punching shear resistance. Four machine learning (ML) algorithms (SVR, DT, RF, and XGBoost) with Bayesian optimization (BO) are presented in this paper to provide accurate predictions for flat slabs. The adoptability and optimization of the models are achieved through the analysis of a database of 337 test specimens with nine design parameters. Machine learning (ML) techniques are used to estimate punching shear resistance, which is compared with design provisions and equations relating to critical shear crack theory (CSCT). According to this study, Bayesian optimization is still capable of improving the performance of conventional machine learning algorithms, while the XGBoost-based model offers advanced capabilities. Predictions based on BO-XGBoost are in good agreement with actual values (*MAE*, *RMSE*, and R^2 are 0.09 MN, 0.14 MN, and 0.92, respectively) in test set. Following a detailed explanation using Shapley additive explanation (SHAP), a high-performance ML approach is used to investigate the predictive results. With the proposed optimized algorithms, it is possible to determine the punching shear resistance of flat slabs with transverse reinforcement during the preliminary stages of the construction.

Keywords Machine learning, Bayesian optimization, Punching shear resistance, RC flat slabs, Transverse reinforcement

1 Introduction

The versatility of flat slabs and the reduced formwork requirements make them a popular option for reinforced concrete (RC) construction (Kang et al., 2021). When punching shear forces are applied to slab-column connections, shear and bending stresses may occur which may result in progressive collapse (refer to Fig. 1). By incorporating transverse reinforcements, it is possible to increase the punching shear resistance. Therefore, its use is encouraged in design codes, including Model Code 2010 (fib MC, 2012). In spite of the widespread use of transverse reinforcement, there is no generally accepted design model that combines accuracy with simplicity. The design codes differ significantly regarding punching resistance, including ACI 318 (ACI Committee, 2019) and Eurocode 2 (EN, 1992-1-1, 2004), or the design parameters have changed over time (i.e., the position of the critical perimeter). It is imperative to realize that many punching strength code provisions are based on empirical models, adjusted to accommodate test results, but without any coherent theory behind them. To extend the validity of the empirical formulae, a growing number of correction factors have been incorporated.

Journal information: ISSN 1976-0485 / eISSN 2234-1315

*Correspondence:
Hua-Jun Yan
19115044@bjtu.edu.cn
[1] School of Civil Engineering, Beijing Jiaotong University, Beijing 100044, China

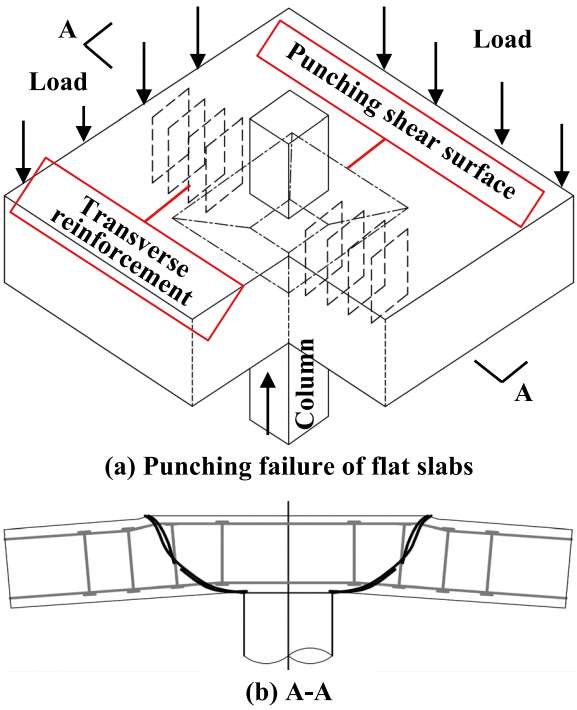

Fig. 1 Flat slabs with transverse reinforcement. **a** Punching failure. **b** A-A

The addition of correction factors does not guarantee safe application when a formula is outside its calibration range (Rankin & Long, 2019), nor does it enable engineers to gain a comprehensive understanding of mechanical behavior.

Thus, researchers have abandoned traditional approaches to correcting empirical formulas in favor of proposing mechanical models applicable to actual conditions. Several studies According to some researchers, concrete slab punching failure is caused by inclined tensile cracks and compressive crushing (Hegger et al., 2009). Choi et al. (2014) presented a method for calculating punching shear strength by assuming that compression is the primary resistance to punching shear at the critical section of the slab. A modification of this model enables it to be applied to both slender and squat concrete footings (Truong & Choi, 2018). However, recent studies have shown that tension resistance must be viewed in conjunction with the interdependent mechanisms of compression and tension shear transfer, which also indicates that tension resistance at critical sections should not be neglected (Ju et al., 2021a, 2021b). Ruiz and Muttoni (2009) proposed the Critical Shear Crack Theory (CSCT), which takes into account all potential shear carrying mechanisms of shear-reinforced slabs. It is assumed that shear-transfer actions are dependent on mechanical parameters such as concrete compressive strength, aggregate size, and crack width. To calculate the failure criteria of the CSCT for slender members, a simplified failure surface and kinematics have been proposed (Muttoni et al., 2017). A limitation, however, is that it results in a discontinuous displacement field along the failure surface (Ruiz et al., 2015; Simoes et al., 2018). The punching resistance of squat slabs and footings is calculated using an effective concrete compressive strength that accounts for crack openings (Cavagnis et al., 2017; Muttoni & Ruiz, 2019). In spite of the fact that all of these researches follow the principles of the CSCT, they have been tailored to address specific problems. Research is being carried out to determine the most effective way to predict punching shear resistance, however, no consensus has yet been reached (Wu et al., 2022).

A number of limitations exist in the models mentioned above, including inadequate consideration of key factors and simplified formulation derivations. Machine learning (ML) has rapidly developed in recent years, providing us with new means of solving complex problems. This method has been applied to civil engineering applications with satisfactory results (Koo et al., 2020; Ngo et al., 2023; Ma et al., 2023) especially when complex boundary conditions are involved. To predict the punching shear resistance of RC flat slabs without transverse reinforcement, multiple ML approaches were applied. Jeong et al. (2021) established prediction models by the K-nearest neighbor (KNN) algorithm, and a database of 104 specimens was compiled by Truong et al. (2022a) to calculate the ultimate strength of slabs, which demonstrated that ML-based models were reliable and accurate for slab evaluation. Further analysis of the punching shear strength was conducted using generative adversarial network (GAN), decision tree, gradient boosting, artificial neural network, deep learning, and random forest (Kim et al., 2022; Shen et al., 2022a, 2022b, 2022c; Truong et al., 2022a, 2022b; Badra et al., 2022; Derogar et al., 2022; Silva et al., 2023). A comparison of these researches with the existing design codes showed that the ML models performed much better than existing methods. However, an accurate model relies on a large dataset (Jumaa & Yousif, 2018). Due to the lack of optimization of parameters, the above methods may have produced overfitted or inaccurate results (Alam et al., 2021). Performance of analysis can be improved through the use of a variety of hyperparameter tuning methods, including grid search (Todorov & Billah, 2022), random search (Liu et al., 2022), and Bayesian optimization (Pan et al., 2022). In contrast to other techniques, Bayesian optimization algorithm select the most appropriate parameter set by optimizing rather than picking one at random (Zhang et al., 2021; Li et al., 2023). In this respect, it may be useful for the analysis of large amounts of complex data. The ML-based models

have proved to be one of the most effective methods for strength predictions, they are still a black box that requires manual input (Shen et al., 2022a, 2022b, 2022c). Several studies have attempted to overcome the difficulty of interpreting ML algorithms by incorporating Shapley additive explanation (SHAP) (Almustafa & Nehdi, 2022; Tran et al., 2022; Feng et al., 2023), Partial dependence plot (Liang et al., 2022), and Eureqa (Faridmehr et al., 2022). Despite the extensive studies of interpretable methods based on the theories above (Ribeiro et al., 2016; Shrikumar et al., 2016), no study has explored the punching shear resistance of RC flat slabs with transverse reinforcement. The behavior of RC flat slab connections may be better understood by an ML-based model with interpretable results.

Up to this point, ML-based approaches have not been developed for predicting ultimate resistance or optimizing the parameters of RC flat slabs with transverse reinforcement. This paper addressed these limitations by identifying geometry and mechanism factors that contribute to failure resistance. It also optimized the model's hyperparameters using Bayesian optimization, and utilized SHAP to interpret the complicated behavior. A comparison of ML algorithms with existing equations provided futher evidence of their superior performance.

After the introduction, the paper is organized as follows: Sect. 2 provides an overview of machine learning algorithms. In Sect. 3, 337 test specimens are divided into two groups (training set and test set) in order to support the ML-based models with Bayesian optimization. In Sect. 4, ML predictions are compared to existing methods along with an explanation provided by SHAP. Lastly, Sect. 5 concludes the study.

2 Methodology

2.1 A Brief Overview of Standard Algorithms

2.1.1 Support Vector Regression (SVR)

An algorithm known as Support Vector Regression (SVR) is used in supervised learning for the purpose of locating a regression plane in which all the sample points lie as close to the regression plane as possible (Scholkopf et al., 2021). To predict the regression, the SVR uses linear functions in a high dimensional space. Through the use of a loss function, the SVR minimizes the risk associated with regression estimation. It is capable of learning from large data sets and is robust to outliers (Sabzekar & Hasheminejad, 2021).

2.1.2 Decision Tree (DT)

Decision tree (DT) model (Bouras & Li, 2023) represent decisions and their consequences in a tree-like structure, in which every internal node represents a decision based on a specific feature, and each leaf node represents a predicted result. It is widely used in practice due to its simplicity and interpretability.

2.1.3 Random Forest (RF)

Random forest (RF) fabricated from decision trees is found to be more effective in bagging than individual algorithms, and often the RF is typically constructed using regression or classification trees as basis estimators (Schonlau & Zou, 2021). Instead of maximizing the metrics for attributes in the regression tree growth process, the RF determines what is the most appropriate solution among the attributes drawn. Using a simple model structure may result in inaccurate predictions, whereas using a complex model structure may result in overfitting. With more features and less overfitting, RF is faster, and can handle high-dimensional data well.

2.1.4 Extreme Gradient Boosting (XGBoost)

The extreme gradient boosting (XGBoost) is a very efficient and powerful boosting learning algorithm (Chen et al., 2023), which introduces several noteworthy improvements within the gradient boosting framework. As a consequence of the XGBoost, the objective function is further enhanced by including a risk factor in order to close the gap between accuracy and complexity and prevent overfitting (Khan et al., 2023). Through this metric, the decision branch grows toward a more obvious overall structure. The XGBoost algorithm is used to continuously optimize the structure and parameters of the model through an objective function, which in turn leads to more accurate predictions.

2.2 Bayesian Optimization (BO) Algorithm

An important aspect of supervised learning is the bias-variance tradeoff (Bayar & Bilir, 2019; Su et al., 2021). A well-tuned set of hyperparameters is crucial for ML models to achieve high cross validation accuracy. Grid-search and random-search methods are used to enumerate the parameters that have changed in optimizations (Nguyen et al., 2021). It should be noted, however, that both methods require extensive programming skills and are generally slow when dealing with large data sets (Liang et al., 2021). For maximum prediction accuracy, Bayesian optimization (BO) is proposed as an alternative to grid-searching and random-searching. Gaussian process (GP) regression is used to determine prior functions, while expected improvement (EI) regression is used to determine acquisition functions. A flowchart of the BO algorithm can be found in Fig. 2, and the covariance kernel can be expressed as follows in GP:

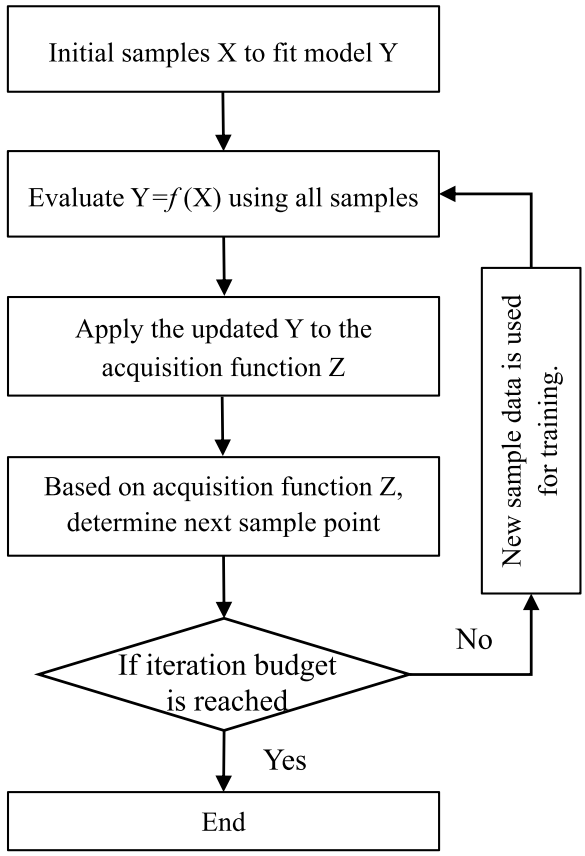

Fig. 2 Flowchart of Bayesian optimization

$$K = \begin{bmatrix} k(X_1, X_1) & \cdots & k(X_1, X_n) \\ \vdots & \ddots & \vdots \\ k(X_n, X_1) & \cdots & k(X_n, X_1) \end{bmatrix} + \sigma_{noise}^2 I \tag{1}$$

where k is the covariance function, n is the sample size, K is corrupted by noise with zero mean and standard deviation (σ_{noise}).

According to this assumption, each observation in sample Y_{n+1} has a Gaussian distribution, and together with the observations in the first n iterations can be considered as a joint Gaussian distribution as follows (Seeger, 2004):

$$Y_{n+1}|D_{1:n} \sim N[\mu(X_{n+1}), \sigma^2(X_{n+1}) + \sigma_{noise}^2] \tag{2}$$

where

$$\mu(X_{n+1}) = k^T (K + \sigma_{noise}^2 I)^{-1} Y_{1:n} \tag{3}$$

$$\sigma^2(X_{n+1}) = k(X_{n+1}, X_{n+1}) - k^T (K + \sigma_{noise}^2 I)^{-1} k \tag{4}$$

$$k = [k(X_{n+1}, X_1) k(X_{n+1}, X_2) \cdots k(X_{n+1}, X_n)] \tag{5}$$

Expect Improvement (EI) is implemented as follows (Jones et al., 1998):

$$EI(X_n) = [y_{best} - \mu(X_n)]\Phi\left(\frac{y_{best} - \mu(X_n)}{\sigma(X_n)}\right) + \sigma(X_n)\varphi\left(\frac{y_{best} - \mu(X_n)}{\sigma(X_n)}\right) \tag{6}$$

A standard Gaussian distribution has two components: a cumulative distribution function (Φ) and a probability distribution function (ϕ), according to the sample space, y_{best} might be the tentative optimal value. In turn, the EI function is more significant at times when the posterior mean is large and the credible interval is wide, thereby preventing an accumulation of information.

2.3 Shapley Additive Explanations (SHAP)

By leveraging additive feature attribution, SHAP intends to examine ML-based models in a mathematically interpretable manner. In the case of a model with input variables $x = (x_1, x_2, \ldots, x_n)$, an original model $f(x)$ can be written as follows:

$$f(x) = g(x') = \phi_0 + \sum_{i=1}^{M} \phi_i x_i' \tag{7}$$

where $g(x')$ stands for explanation model, amount of input features indicated by M, ϕ_0 is the value that is obtained when all inputs are missing. Based on Lundberg & Lee (2017), Eq. (7) may be solved as:

$$\phi_i(f, x) = \sum_{z' \subseteq x'} \frac{|z'|!(M - |z'| - 1)!}{M!} [f_x(z') - f_x(z' \backslash i)] \tag{8}$$

where $|z'|$ means the number of entries that are not zero in z'; $f_x(z') = f[h_x(z')] = E[f(z) \mid z_s]$. There are a number of input variables that can have a positive or negative impact on a prediction through SHAP method, further detailed explanations refer to the reference (Mangalathu et al., 2020).

3 Analysis of Flat Slabs with Transverse Reinforcement

3.1 Existing Models for Resistance Prediction

In this section, two design codes (ACI 318-19, Eurocode 2) and a mechanical model (CSCT) were used to predict the punching shear resistance of flat slabs with transverse reinforcement.

3.1.1 ACI 318 Code

In accordance with ACI 318-19 (ACI Committee, 2019), the punching shear strength is defined as follows:

$$V_{Rk,\max} = 0.5\lambda_s \sqrt{f_c'}\, b_0 d \tag{9}$$

$$V_{Rk,cs} = 0.17\lambda_s \sqrt{f_c'}\, b_0 d + \frac{A_{sw} f_{ywt} d}{S_r} \tag{10}$$

$$V_{Rk,out} = 0.17\lambda_s \sqrt{f_c'}\, b_{0,out} d \tag{11}$$

$$\lambda_s = \sqrt{\frac{2}{1+0.004d}} \le 1 \tag{12}$$

where b_0 is a perimeter located $0.5d$ away from the column face, d refers to the effective slab depth, f_c' represents the compressive strength of concrete cylinders, f_{ywt} is the yield stress of shear reinforcements, A_{sw} stands for the area of one layer of shear reinforcements, S_r is the distance between the shear reinforcements, $b_{0,out}$ is the critical perimeter which is located at $0.5d$ from the last layer of shear reinforcements.

3.1.2 Eurocode 2

Based on Eurocode 2 (EN 1992-1, 2004), the punching shear strength for flat slabs with transverse reinforcement can be calculated as follows:

$$V_{Rk,\max} = 0.24\left(1 - \frac{f_c}{250}\right) f_c\, b_0\, d \tag{13}$$

$$V_{Rk,cs} = 0.135k(100\rho f_c)^{\frac{1}{3}} b_0 d + 1.5\frac{A_{sw} f_{yw,ef}\, d}{S_r} \tag{14}$$

$$V_{Rk,out} = 0.18k\left(100\rho f_c\right)^{\frac{1}{3}} b_{0,out} d \tag{15}$$

$$k = \left(1 + \sqrt{\frac{200}{d}}\right) \le 2 \tag{16}$$

where k stands for the size effect, ρ refers to the ratio of flexural reinforcement, $f_{yw,ef}$ represents the effective strength of the shear reinforcement.

3.1.3 Critical Shear Crack Theory (CSCT)

It has been proposed that punching shear failure happens when a shear crack opens on a slab of concrete, as described in the CSCT (Muttoni & Ruiz, 2019; Ruiz & Muttoni, 2009). This theory assumes that the crack opening is proportional to the amount of rotation the slab experiences outside of the column region. In order to determine the slab load-rotation relationship, the following equation can be used:

$$\psi = 1.5\frac{r_s}{d}\frac{f_y}{E_s}\left(\frac{V/8}{m_R}\right)^{1.5} \tag{17}$$

where V represents the shear force; r_s is the slab's radius; m_R represents the moment of resistance. In order to calculate the failure load for a slab that is rotating, the following failure criteria must also be taken into account:

$$V_R(\psi) = \frac{3}{4}\frac{b_{0,CSCT} d\sqrt{f_c}}{1 + 15\frac{\psi d}{d_{g0}+d_g}} + \sum_{i=1}^{n} \sigma_{st,i}(\psi) A_{v,i} \tag{18}$$

$$V_{R,\max}(\psi) = \lambda\frac{3}{4}\frac{b_{0,CSCT} d\sqrt{f_c}}{1 + 15\frac{\psi d}{d_{g0}+d_g}} \tag{19}$$

where d_g represents the maximum aggregate size; d_{g0} refers to the size of the reference aggregate; $b_{0,CSCT}$ is the control perimeter set to $0.5d$ around the support region; A_v refers to the shear reinforcement's cross-section; σ_{st} refers to the stress that is developed during a rotation of a given direction; λ is a coefficient that depends on the type of shear reinforcement system.

3.2 Database of Flat Slabs with Transverse Reinforcement

3.2.1 Data Collection

As part of this study, independent datasets were derived from laboratory experiments performed on a slab-column connection with transverse reinforcement. During this study, only slabs with punching shear failures were considered. Thus, the dataset accurately represents the performance of slab-column connections with shear reinforcement under punching-shear failure mode, facilitating the investigation of the factors that affect punching shear resistance. Three hundred and thirty-seven 337 experimental data points (CEP-FIP, 2001; Stein et al., 2007; Rojek & Keller, 2007; Ferreira et al., 2014; Walker, 2014; Bartolac et al., 2015; Jin et al., 2017; Dam et al., 2017; Eom et al., 2018; Jang & Kang, 2021; Cantone et al., 2019; Jin et al., 2019; Lewinski & Wiech, 2020; Said et al., 2020; Lima et al., 2020; Oliveira et al., 2022; Shatarat & Salman, 2022) were obtained from published articles containing various types of axially symmetrically loaded interior columns. Most slab-column tests involve a single column, often referred to as an isolated slab-column connection. The slab portion dimensions should represent the contraflexure points or negative moment zones. Among the major advantages of single column tests is the ability to test full-scale specimens. In this way, the shear stresses are not influenced by the size effect, which leads to continuous reductions in shear strength with increase in slab depth. In spite of this, they fail to adequately simulate the behavior of a slab-column connection in a real

structure and do not take into account boundary conditions, confinement, and in-plane forces. Furthermore, load redistribution is impossible. It is shown in Fig. 3 that the parameters fall within a certain range, and a distribution of the parameter values is provided in Appendix. In which a is the distance from the column face to the moment inflection point of a slab (called shear span), d is the effective depth, c is the equivalent column width (circular cross-section is converted to a square cross-section in ACI 318-19), ρ_t is the flexural reinforcement ratio, b_0 is the critical perimeter located at $0.5d$ from the column face, $A_{sw,d}$ represents the shear reinforcement cross section area within d from the column face, f_{lc} stands for the compressive strength of the concrete ($\phi = 150$ mm, $h = 300$ mm), f_y is the yield strength of the flexural reinforcement, $f_{y,sw}$ is the yield strength of the shear reinforcement. In most researches, bent up bars (BuB), stirrups (Sti), hooks (Ho), stud rails (StR), shear ladders (ShA), shear bonds (SB), and double headed studs (DHS) are used as shear reinforcement. According to Fig. 3, this dataset contains a wide variety of concrete strength and reinforcement data. To develop models that predict punching shear resistance accurately in a wide range of real-world situations, it is critical to gather this information. Also, the resistance values demonstrated a wide range of punching shear strengths, suggesting that the dataset represents a variety of load conditions. According to some studies (Faridmehr et al., 2022; Liang et al., 2022; Mangalathu et al., 2021), similar data sizes are capable of providing good prediction results.

3.2.2 Variable Definitions for Inputs and Outputs

Data-driven models were used in ML algorithms to predict outcomes. However, they are based on an enormous amount of data, disregarding prior knowledge of mechanisms. Data collection for engineering problems can be a difficult and labor-intensive process due to the amount of work involved. For ML approaches to be accurate and predictive, knowledge of mechanics is required. Table 1 shows the input and output variables, including mechanics-features: flexural ($\rho_t f_y$) and shear ($A_{sw,d} f_{y,sw}$) reinforcement contributions; a root square of concrete compressive strength ($\sqrt{f_{lc}}$).

3.2.3 Normalization

The goal of normalization is to scale features on a similar basis. Normalization is a common method incorporated into gradient descent algorithms (Taffese & Espinosa-Leal, 2022). It's controlled between [0,1] for uniform transformation processing of input data. As a means of reducing the statistical bias of parameters and improving the reliability of the ML models, the following normalization procedure may be used:

$$X_{i,normalized} = \frac{X_i - X_{\min}}{X_{\max} - X_{\min}} \tag{20}$$

where $X_{\min}$ and $X_{\max}$ are the minimum and maximum values of one class of input values, respectively.

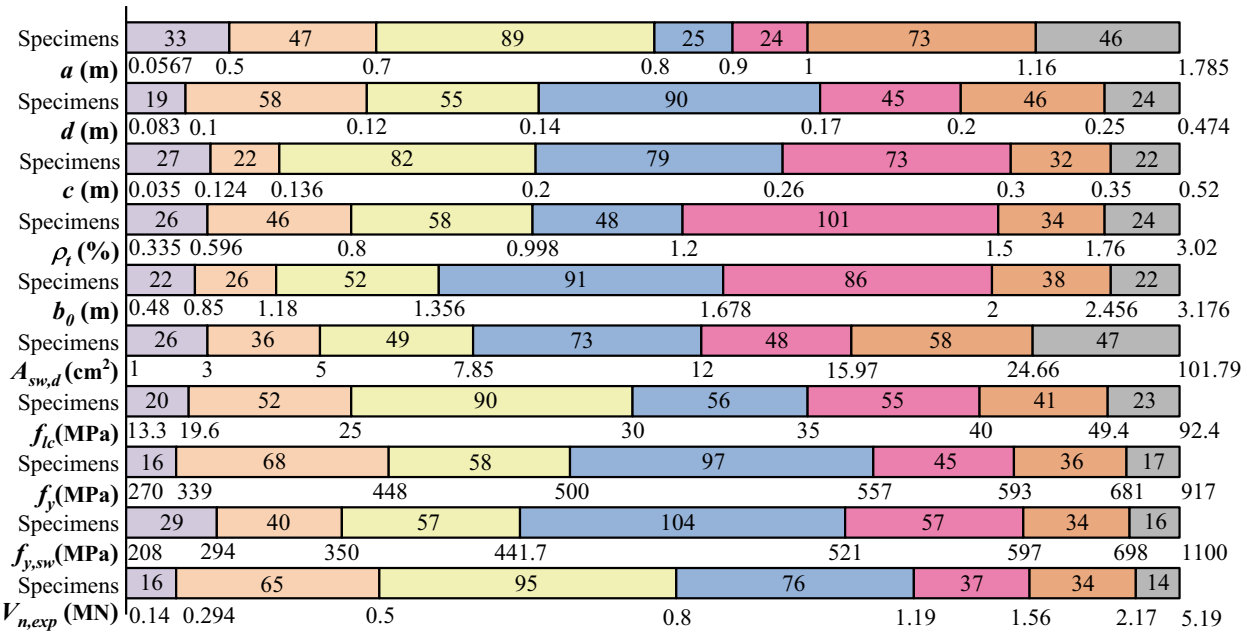

Fig. 3 Experimental distributions of features

Table 1 Statistical summary of variables

Input/output	Parameters	Notation	Units
Input	x_1: Effective depth of the slab	d	(m)
Input	x_2: Span to effective depth ratio	a/d	(–)
Input	x_3: Column width to critical perimeter ratio	c/b_0	(–)
Input	x_4: A root square of concrete compressive strength	$\sqrt{f_{lc}}$	(–)
Input	x_5: Contribution of the flexural reinforcement	$\rho_t f_y$	(MPa)
Input	x_6: Contribution of the shear reinforcement	$A_{sw,d} f_{y,sw}$	(MN)
Output	y: Failure load	$V_{n,exp}$	(MN)

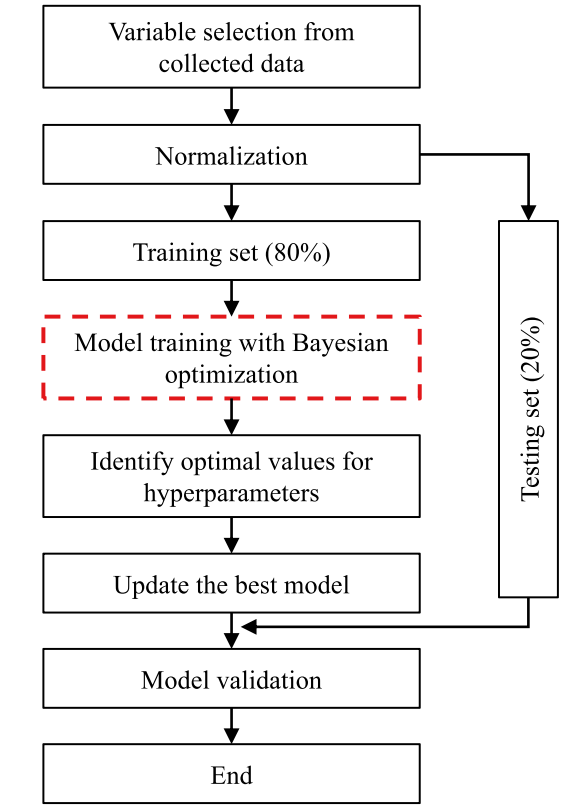

Fig. 4 Flowchart for the learning algorithms with BO

3.3 Development of ML Models

In this paper, ML models are implemented using fully automated Bayesian optimization for flat slabs with transverse reinforcement. To train four standard models (SVR, RF, DT, and XGBoost), features were used without selecting anything artificially. An optimization algorithm based on Bayesian theory is then used to optimize selected features. A random partition of the dataset is made into training set and test set after normalization, which comprise 80% and 20% of the overall database, respectively (refer to Fig. 4). Data from test set (20%), which have not been used in the training process, is used to validate the accuracy and reliability of the model.

3.4 Measurement of Performance

Several statistical variables can be used to evaluate predictive models' efficiency, including coefficient of determination R^2, mean absolute error (*MAE*), and root mean square error (*RMSE*). Generally, the prediction model is considered more accurate if R^2 approaches one, while *MAE* and *RMSE* decline and approach zero, respectively. Measures of performance are expressed as follows:

$$R^2 = 1 - \frac{\sum_{i=1}^{n} \left(y_{n,pre} - y_{n,\exp}\right)^2}{\sum_{i=1}^{n} \left(y_{n,\exp} - \frac{1}{n}\sum_{i=1}^{n} y_{n,\exp}\right)^2} \tag{21}$$

$$MAE = \frac{1}{n}\sum_{i=1}^{n} \left|y_{n,pre} - y_{n,\exp}\right| \tag{22}$$

$$RMSE = \sqrt{\frac{1}{n}\sum_{i=1}^{n} \left(y_{n,pre} - y_{n,\exp}\right)^2} \tag{23}$$

where $y_{n,pre}$ is the predicted value, while $y_{n,exp}$ is the experimental result.

4 Results and Discussions

4.1 Comparison of Model Performance

An optimal set of hyperparameters was found after 50 iterations (refer to Fig. 5), and the parameters of the ML algorithms are listed in Table 2. According to the BO's objective function, its results are based on the averaged R^2 of iterations, which results in:

$$x_{best} = \arg\max f(x) \tag{24}$$

where f is defined as the function, and x_i is the input variable in each ML model.

A statistical analysis of the predicted output is provided in Table 3. There is no doubt that training is more

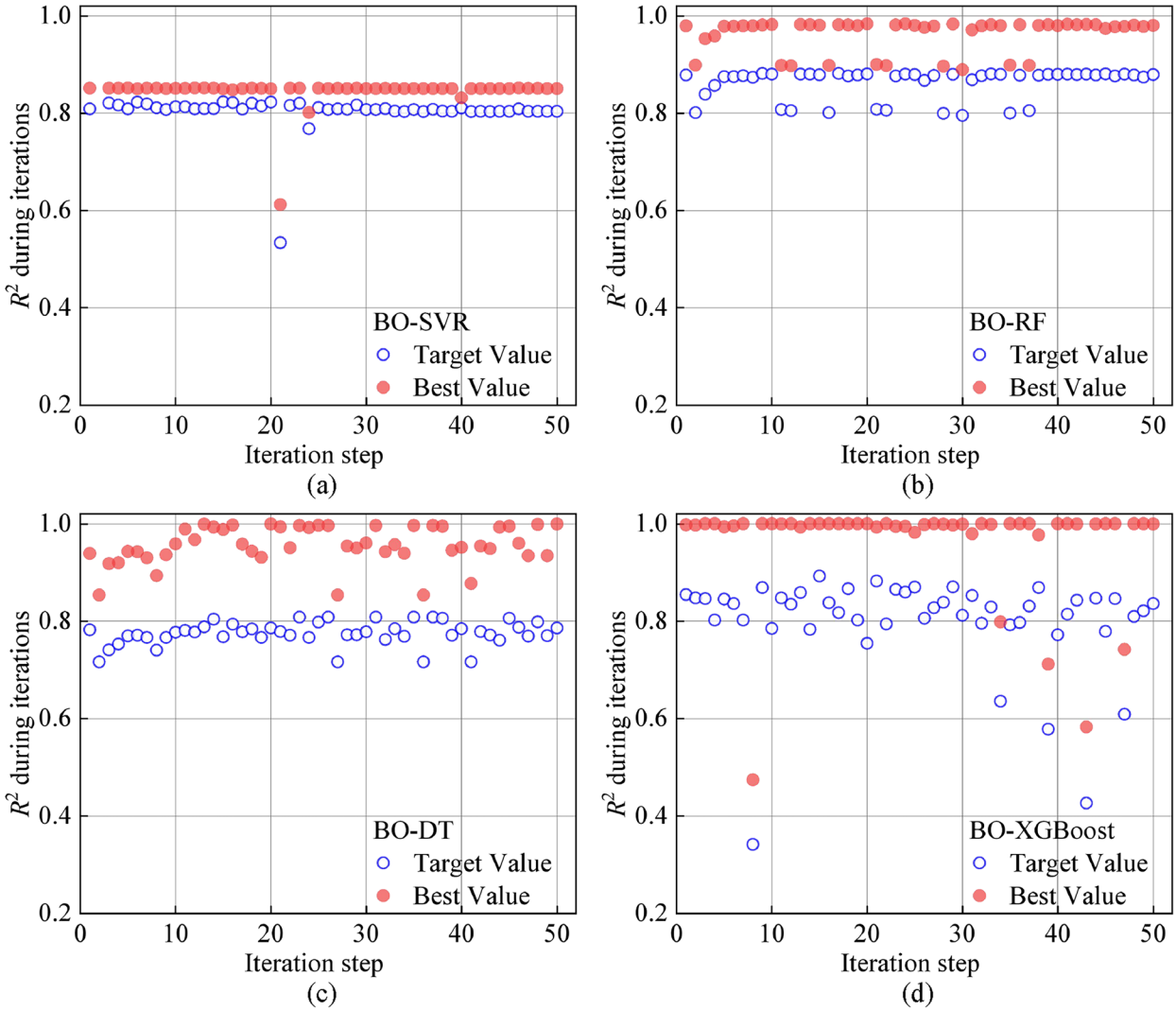

Fig. 5 R^2 history of BO: **a** BO-SVR. **b** BO-RT. **c** BO-DT. **d** BO-XGBoost

Table 2 The main parameters of comparison models

Algorithm	Initial basic parameters	After Bayesian optimization
SVR	C = 1; gamma = 1; kernel = 'linear'; degree = 3; coef0 = 0; tolerance = 1e-3; C = 1; epsilon = 0.1, shrinking = True	C = 0.96; gamma = 3.75; kernel = 'linear'; degree = 3; coef0 = 0; tolerance = 1e-3; C = 1; epsilon = 0.1, shrinking = True
RF	n of estimators = 20; max depth = 3; criterion = "squared error"; min samples split = 2; min samples leaf = 1; random state = 1	n of estimators = 157; max depth = 15; criterion = "squared error"; min samples split = 2; min samples leaf = 1; random state = 1
DT	Criterion = mse; splitter = best; min sample leaf = 1; min samples split = 2; max depth = 3; max features = None; Random state = None; ccp alpha = 0.0	Criterion = mse; splitter = best; min sample leaf = 1; min samples split = 13; max depth = 4; max features = None; Random state = None; ccp alpha = 0.0
XGBoost	n estimators = 20; learning rate = 0.1; max depth = 3; objective = 'linear'; booster = 'gbtree'; min child weight = 1; subsample = 1; colsample bytree = 1; alpha = 0; lambda = 1	n estimators = 238; learning rate = 0.257; max depth = 4; objective = 'linear'; booster = 'gbtree'; min child weight = 1; subsample = 1; colsample bytree = 1; alpha = 0; lambda = 1

Table 3 Performance comparison of prediction models

ML models	R^2		*MAE* (MN)		*RMSE* (MN)	
	Training	Test	Training	Test	Training	Test
SVR	0.85	0.80	0.16	0.15	0.26	0.22
RF	0.89	0.76	0.15	0.18	0.22	0.24
DT	0.87	0.72	0.16	0.19	0.24	0.26
XGBoost	0.90	0.82	0.14	0.14	0.22	0.21
BO-SVR	0.85	0.80	0.16	0.15	0.26	0.22
BO-RF	0.98	0.90	0.048	0.10	0.094	0.15
BO-DT	0.992	0.89	0.033	0.11	0.059	0.16
BO-XGBoost	0.999	0.92	0.003	0.091	0.005	0.14

accurate than testing, in which case testing is an exact representation of the model's performance. As far as prediction results are concerned, BO-XGBoost performs well in both training and testing sets, with R^2, *MAE*, and *RMSE* of 0.92, 0.091 MN, and 0.14 MN in the test set, respectively.

In comparison with the original standard algorithms, BO models obtained a larger correlation coefficient (R^2) and a smaller error metric (*MAE*, *RMSE*) than the original standard algorithms. According to this study, Bayesian optimization is still capable of improving the performance of conventional machine learning algorithms, while the XGBoost-based model offers advanced capabilities.

4.2 Comparison with Design Codes and CSCT Equations

According to Fig. 6, the proposed model is compared to three existing models that have already been developed. In Table 4, the precision and reliability of the capacity estimated through a model was assessed by comparing the actual resistance with the resistance determined by the model ($V_{n,exp}$ / $V_{n,pre}$). Fig. 6 a-c shows that the two design codes and the equation for CSCT skew conservatively, especially for ACI 318 code. A possible limitation is that only Eurocode 2 and CSCT consider the effect of flexural reinforcement ratio ρ_t on resistance. Additionally, the CSCT takes into account the yield strength of flexural reinforcement f_y. According to some studies (Derogar et al., 2022; Liang et al., 2022), their absence can lead to a reduction in accuracy. Due to safety requirements, the coefficients in the design codes are modified while they are not for the mechanical model (CSCT) (Tian et al., 2009; Enipaul et al., 2015; Deifalla, 2021). If the model is not revised, prediction errors may result as evidenced by punching shear resistances exceeding 1000 kN.

A comparison of the models suggests that they were over-simplified, and some influential factors need to be considered. In Fig. 6d–k, scatter plots of ML models in training and test sets are illustrated in order to visualize prediction outcomes. As shown in Fig. 6d-k, conventional ML algorithms (SVR, RF, DT, and XGBoost) produce a large predicted deviation, and their dispersion degrees are much greater than those obtained following Bayesian optimization.

The comparison in Table 4 shows BO-XGBoost to have the best prediction performance among all the models, with the highest R^2 (0.92), lowest *MAE* (0.091 MN), *RMSE* (0.14 MN), and COV (0.13) in test set. Based on comparisons between the BO-XGBoost model and Eurocode 2, which is considered to be the most precise model among the design equations (Magalathu et al., 2021), *RMSE* values and *MAE* values are significantly reduced by 46.2% and 46.5%, respectively.

This is due to the fact that BO-XGBoost takes into account all input variables that could affect the strength of shear reinforced slabs, which are well optimized by BO. The mechanics of failure resistance ($\sqrt{f_{lc}}$, $\rho_t f_y$, and $A_{sw,d} f_{y,sw}$) and the geometric properties (d, a/d, and c/b_0) of slabs must be considered in order to calculate the response of real structures. In light of the limitations of the existing equations, ML-based models may be able to solve the problem of predicting punching shear resistance.

4.3 SHAP-Based Importance Factor Indentification

Despite its high predictive accuracy, the BO-XGBoost model generally behaves as a black-box, unable to interpret the relationship between input variables and resistance. It is possible to interpret several parameters with a BO-XGBoost model using SHAP, which has also been confirmed in other studies (Mangulathu et al., 2021; Liang et al., 2022).

4.3.1 SHAP Values

An integral measure of the significance of a feature is the SHAP value. A Shapley value is a conditional expectation

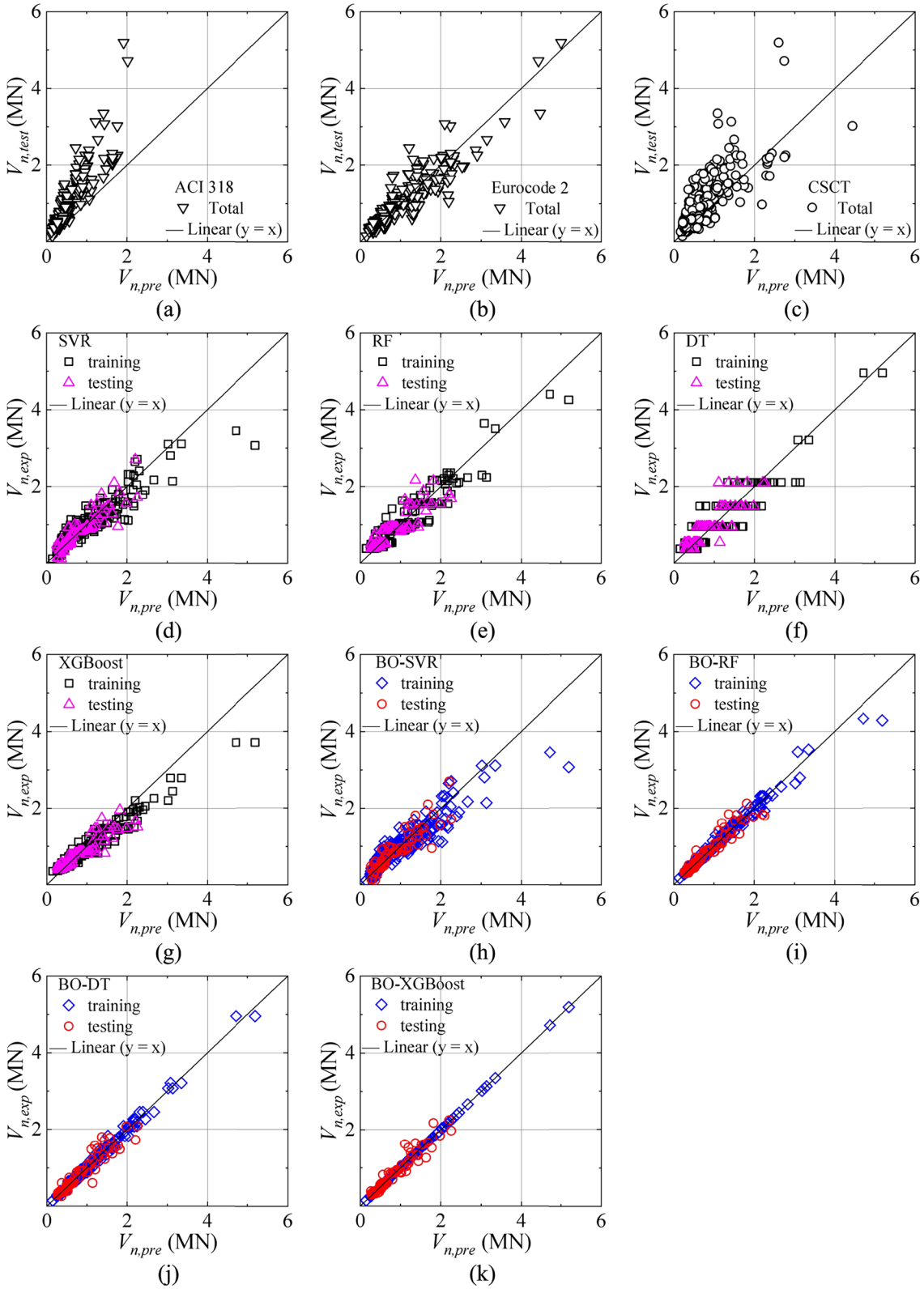

Fig. 6 Comparison with existing strength models. **a** ACI 318-19. **b** Eurocode 2. **c** CSCT. **d** SVR. **e** RF. **f** DT. **g** XGBoost. **h** BO-SVR. **i** BO-RF. **j** BO-DT. **k** BO-XGBoost

Table 4 Results of the comparison

Equations	AVG ($V_{n,exp}/V_{n,pre}$)	COV ($V_{n,exp}/V_{n,pre}$)	*MAE* (MN)	*RMSE* (MN)	R^2
ACI 318	1.84	0.23	0.42	0.56	0.65
Eurocode 2	1.09	0.22	0.17	0.26	0.84
CSCT	1.41	0.41	0.32	0.48	0.46
SVR (test)	1.07	0.36	0.15	0.22	0.80
RF (test)	0.95	0.25	0.18	0.24	0.76
DT (test)	0.95	0.29	0.19	0.26	0.72
XGBoost (test)	0.99	0.22	0.14	0.21	0.82
BO-SVR (test)	1.07	0.35	0.15	0.22	0.80
BO-RF (test)	0.98	0.14	0.10	0.15	0.90
BO-DT (test)	1.01	0.18	0.11	0.16	0.89
BO-XGBoost (test)	0.99	0.13	0.091	0.14	0.92

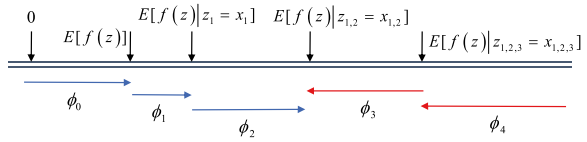

Fig. 7 SHAP values

function, which is a solution to Eq. 8. In Fig. 7, Each SHAP value represents the change in the anticipated model prediction when that feature is conditioned on. In the case of nonlinear models or features that are not independent, the features are added to the underlying expectation, and the SHAP value (V_{SHAP}) is calculated by averaging the individualϕ_i values.

4.3.2 Global Interpretations

As the most reliable model for interpretation by the SHAP method, BO-XGBoost is selected for this section. This figure (Fig. 8a) illustrates the importance factors for input variables, ranked in accordance with their impact on prediction results. One should note that the slab's effective depth (d), whose SHAP value is 0.39, is the most significant. A second critical feature was the shear reinforcement ($A_{sw,d}\,f_{y,sw}$), with a SHAP value of 0.11, which contributed approximately 28% of the d, roughly twice as

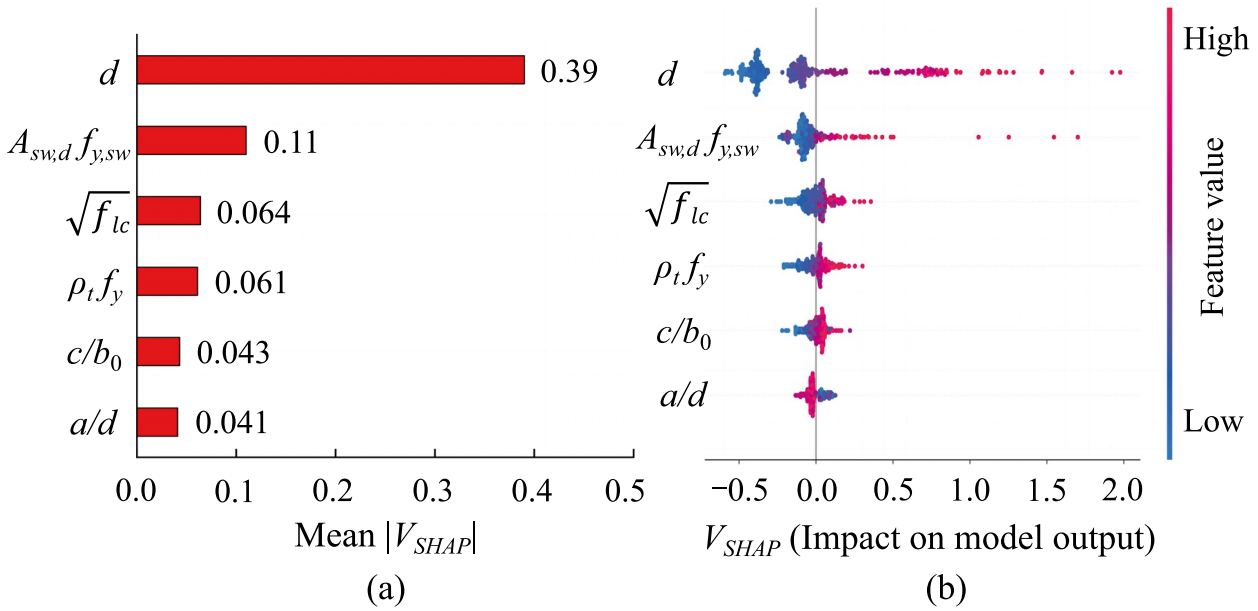

Fig. 8 Global interpretations. **a** Feature importance of input variables. **b** The summary of SHAP values

much as $\sqrt{f_{lc}}$ and $(\rho_t f_y)$. This also indicates that increasing the contribution of shear reinforcement $(A_{sw,d} f_{y,sw})$ can have double impact than enhancing the strength of concrete $(\sqrt{f_{lc}})$ and flexural reinforcement $(\rho_t f_y)$. There are SHAP values of 0.043 and 0.041 for (c/b_0) and (a/d), although their importance is low, they cannot be ignored.

There is an apparent lack of clarity in Fig. 8a regarding whether each parameter affects prediction positively or negatively, but this can be clarified by examining the SHAP summary plots, as shown in Fig. 8b. On a scale from small to large, each variable is colored blue or red. Input variables (d, $A_{sw,d} f_{y,sw}$, $\rho_t f_y$, $\sqrt{f_{lc}}$, and c/b_0) are considered to have a positive impact on prediction results. As a result, flab slabs with high values on these five input variables are more likely to get higher punching shear resistance. In addition, the impact of (a/d) is not significant, but can still be considered as a negative factor.

4.3.3 Feature Dependency

By examining the relationship between a particular variable and its most closely related factors, it is also possible to explain BO-XGBoost's prediction mechanism based on SHAP. A higher SHAP value indicates an improvement in punching shear resistance. The results of this analysis (refer to Fig. 9) show that SHAP values increase with additional values for variables d, (c/b_0), $(\sqrt{f_{lc}})$, $(\rho_t f_y)$, and $(A_{sw,d} f_{y,sw})$, respectively, and decrease with increasing value of (a/d).

The influence of d on punching shear resistance has also been determined through experimental researches (Muttoni & Ruiz, 2019; Pang et al., 2021). In the case of a slab whose effective depth increases from 100 to 400 mm, the SHAP value increases from (− 0.5) to (+1.5), and its rate increases is much faster than other parameters (Fig. 9a), especially when the d exceeds 180 mm, it has an positive effect on the punching capacity. Also, calculations using the design codes show that ACI 318-19 and EC2-2004 provide unconservative predictions for slabs with d greater than 200 mm, but provide improved predictions for slabs with d less than 200 mm (Derogar et al., 2022). Furthermore, it is evident from the results that standard calculation methods are incapable of identifying precisely the contribution of parameter d, while ML-based models can provide a clearer explanation of the relationship between parameters and outcomes, along with the ability to continuously improve the formula.

In spite of the fact that increasing d can enhance the resistance of slabs, it can also increase the risk of brittle punching failures. A common design approach for improving punching shear capacity is to use transverse reinforcements (Oliveira et al., 2021; Shatarat & Salman, 2022). As the $(A_{sw,d} f_{y,sw})$ between 0 and 5 MN, the SHAP value increases from (− 0.25) to (+1.25), in which the punching resistance increases only if the shear reinforcement contributes more than 1 MN (Fig. 9f).

The SHAP value decreases from (+0.3) to (− 0.2) with the concrete compressive strength decreasing from 80 to 20 MPa (Fig. 9d). There may be a reason for this, that concrete crack sizes and widths increase with decreasing concrete strength in punching shear loads. It is generally accepted that larger cracks in concrete reduce its capability of transferring shear, due primarily to the reduced possibility of interlocking between aggregate grains on opposite sides of the shear crack. The failure of slabs in punching shear is more likely to occur when the f_{lc} increases (Hallgren, 1996), maybe because the steel bar yields before the slab fails. These results are also consistent with those reported in this study.

There is no doubt that $(\rho_t f_y)$ has a positive impact on the flat slabs, however it should be noted that previous literature (Elstner & Hognestad, 1956; Faridmehr et al., 2022) indicated that when the value of ρ_t is very small, the slab will fail before the shear reinforcement has fully worked. Fig. 9e indicates that SHAP will be greater than zero only when $(\rho_t f_y)$ is greater than 6 MPa, which will result in a positive impact on punching shear resistance. A possible explanation is that when the flexural reinforcement is insufficient, wider cracks may appear inside the slab-column connection, which would result in early failure of the structure and greatly reduce the effectiveness of transverse reinforcement.

The ACI 318-19 and EC2-2004 do not take all (a/d) into account when calculating the punching shear resistance of flat slabs. In Fig. 9b, SHAP value increased from (− 0.10) to (+0.10) while (a/d) decreased from 10 to 2, where (a/d) less than 5 is associated with a positive effect on punching shear resistance. It can be attributed to the development of arch mechanisms in slabs as well as the effects of friction at the support (Lovrovich & Mclean, 1990).

In the case of a slab whose (c/b_0) increases from 0.1 to 0.2, the SHAP value increases from (− 0.2) to (+0.2) (Fig. 9c), especially when the (c/b_0) exceeds 0.14, it has an positive effect on the punching shear resistance. A higher (c/b_0) limits the formation of the punching shear cone, however current design methods often ignore this impact.

In conclusion, the feature importance analysis indicates that the d, (a/d), (c/b_0), $(\sqrt{f_{lc}})$, $(\rho_t f_y)$, and $(A_{sw,d} f_{y,sw})$ played a crucial role in the predictive performance of the optimized model. As noted, different parameters contribute to punching shear resistance to varying degrees within a certain range.

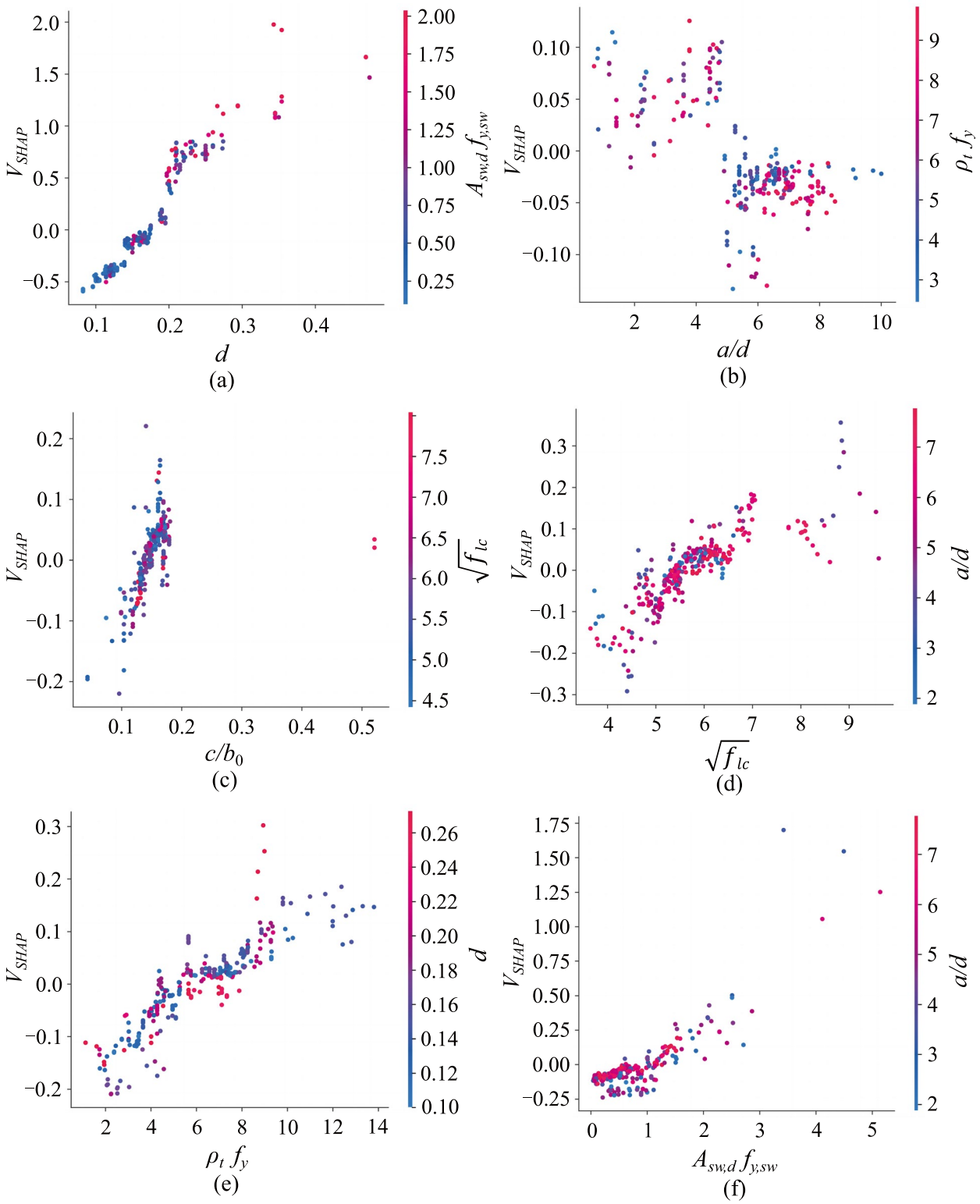

Fig. 9 Dependency plots for features

5 Conclusions

In previous studies, the punching shear resistance of flat slabs with transverse reinforcement was extensively investigated, with a variety of empirical predictions being made. It is possible to reduce bias and variance in these predictions by incorporating mechanics features into data-driven approaches. For this purpose, 337 test results were collected and analyzed using BO hybrid methods based on four common algorithms (SVR, RF, DT, and XGBoost). For accuracy evaluation, the proposed ML-based models were compared to design codes (ACI 318, Eurocode 2) as well as CSCT equations. Results of the analysis allow the following conclusions to be drawn:

(1) While the Eurocode 2 performs better than the ACI 318 and CSCT, it still leaves a considerable gap compared with ML algorithms in terms of calculation results.

(2) As compared to other standard algorithms (SVR, RF, DT), XGBoost achieved optimal results with R^2, *MAE*, and *RMSE* values of 0.82, 0.14MN, and 0.21MN, respectively.

(3) After Bayesian optimization, BO-XGBoost showed significantly lower *RMSE* and *MAE* values than XGBoost by 33% and 35%, respectively, and did not display any obvious bias toward the input variables which is a critical characteristic of an ideal predictive model.

(4) Based on SHAP explanation, the most significant variable affecting punching shear resistance is d, while (a/d) has the least impact and $(A_{sw,d} f_{y,sw})$ can have a double impact compared to $(\sqrt{f_{lc}})$ and $(\rho_t f_y)$. According to this information, the design considerations can be prioritized and the design process can be improved.

(5) This study concentrated on the prediction of punching shear resistance without considering any other failure modes, which may also result in some limitations, such as brittle failure occurring as the value of d increases. The failure modes of flat slabs should therefore be considered in future research.

Supplementary Information

The online version contains supplementary material available at https://doi.org/10.1186/s40069-024-00721-9.

Additional file 1.

Acknowledgements
Not applicable.

Author contributions
Both authors read and approved the final manuscript.

Funding
No funding was received.

Availability of data and materials
All data that support the findings of this study are available from the corresponding author upon reasonable request.

Declarations

Competing intersts
The autors declare no competing interests.

Received: 14 July 2023 Accepted: 9 August 2024
Published online: 05 November 2024

References

ACI Committee 318. (2019). *Building code requirements for structural concrete and commentary (ACI 318–19)*. American Concrete Institute.

Alam, M. S., Sultana, N., & Hossain, S. M. Z. (2021). Bayesian optimization algorithm based support vector regression analysis for estimation of shear capacity of FRP reinforced concrete members. *Applied Soft Computing, 105*, 107281. https://doi.org/10.1016/j.asoc.2021.107281

Almustafa, M. K., & Nehdi, M. L. (2022). Novel hybrid machine learning approach for predicting structural response of RC beams under blast loading. *Structures, 39*, 1092–1106. https://doi.org/10.1016/j.istruc.2022.04.007

Badra, N., Haggag, S. Y. A., Deifall, A., & Salem, N. M. (2022). Development of machine learning models for reliable prediction of the punching shear strength of FRP-reinforced concrete slabs without shear reinforcements. *Measurememt, 201*, 111723. https://doi.org/10.1016/j.measurement.2022.111723

Bartolac, M., Damjanovic, D., & Duvnjak, I. (2015). Punching strength of flat slabs with and without shear reinforcement. *Gradevinar, 67*(8), 771–786. https://doi.org/10.14256/JCE.1361.2015

Bayar, G., & Bilir, T. (2019). A novel study for the estimation of crack propagation in concrete using machine learning algorithms. *Construction and Building Materials, 215*, 670–685. https://doi.org/10.1016/j.conbuildmat.2019.04.227

Bouras, Y., & Li, L. (2023). Prediction of high-temperature creep in concrete using supervised machine learning algorithms. *Construction and Building Materials, 400*, 132828. https://doi.org/10.1016/j.conbuildmat.2023.132828

Cantone, R., Ruiz, M. F., Bujnak, J., & Muttoni, A. (2019). Enhancing punching strength and deformation capacity of flat slabs. *ACI Structural Journal, 116*(5), 261–274. https://doi.org/10.14359/51716842

Cavagnis, F., Ruiz, M. F., & Muttoni, A. (2017). A mechanical model for failures in shear of members without transverse reinforcement based on development of a critical shear crack. *Engineering Structures, 157*, 300–315. https://doi.org/10.1016/j.engstruct.2017.12.004

CEB-FIP. (2001). Punching of structural concrete slabs. *CEB-Bull, 12*, 284p.

Chen, Y. F., Li, F., Zhou, S. Q., Zhang, X., Zhang, S., Zhang, Q., & Su, Y. J. (2023). Bayesian optimization based random forest and extreme gradient boosting for pavement density prediction in GPR detection. *Construction and Building Materials, 387*, 131564. https://doi.org/10.1016/j.conbuildmat.2023.131564

Choi, K. K., Shin, D. W., & Park, H. G. (2014). Shear-strength model for slab-column connections subjected to unbalanced moment. *ACI Structural Journal, 111*(S40), 3. https://doi.org/10.14359/51686533

Dam, T. X., Wight, J. K., & Parra-Montesinos, G. J. (2017). Behavior of monotonically loaded slab-column connections reinforced with shear studs. *ACI Structural Journal, 114*(1), 221–232. https://doi.org/10.14359/51689165

de Oliveira, V. H. D., de Lima, H. J. N., & Melo, G. S. (2022). Punching shear resistance of flat slabs with different types of stirrup anchorages such as shear reinforcement. *Engineering Structures, 253*, 113671. https://doi.org/10.1016/j.engstruct.2021.113671

Deifalla, A. (2021). A comparative study and a simplified formula for punching shear design of concrete slabs with or without membrane tensile forces. *Structures, 33*, 1936–1953. https://doi.org/10.1016/j.istruc.2021.05.070

Derogar, S., Ince, C., Yatbaz, H. Y., & Ever, E. (2022). Prediction of punching shear strength of slab-column connections: A comprehensive evaluation of machine learning and deep learning based approaches. *Mechanics of Advanced Materials and Structures*. https://doi.org/10.1080/15376494.2022.2134950

Einpaul, J., Ruiz, M. F., & Muttoni, A. (2015). Influence of moment redistribution and compressive membrane action on punching strength of flat slabs. *Engineering Structures, 86*, 43–57. https://doi.org/10.1016/j.engstruct.2014.12.032

Elstner, R. C., & Hognestad, E. (1956). Shearing strength of reinforced concrete slabs. *ACI Journal of Process, 100*(8), 1548–1549.

EN 1992-1-1. (2004). Eurocode 2: Design of concrete structure, Part 1–1: General rules and rules for buildings. European Committee for Standardization

Eom, T. S., Kang, S. M., Choi, T. W., & Park, H. K. (2018). Punching shear tests of slabs with high-strength continuous hoop reinforcement. *ACI Structural Journal, 115*(5), 1295–1305. https://doi.org/10.14359/51702231

Faridmehr, I., Nehdi, M. L., & Baghban, M. (2022). Novel informational bat-ANN model for predicting punching shear of RC flat slabs without shear reinforcement. *Engineering Structures, 256*, 114030. https://doi.org/10.1016/j.engstruct.2022.114030

Fédération internationale du béton (fib). (2012). fib model code for concrete structures 2010. fib Bulletin 65. Lausanne. Switzerland

Feng, J. P., Zhang, H. W., Gao, K., Liao, Y. C., Yang, J., & Wu, G. (2023). A machine learning and game theory-based approach for predicting creep behavior of recycled aggregate concrete. *Case Studies in Construction Materials, 17*, e01653. https://doi.org/10.1016/j.cscm.2022.e01653

Ferreira, M. P., Melo, G. S., Regan, P. E., & Vollum, R. L. (2014). Punching of reinforced concrete flat slabs with double-headed shear reinforcement. *ACI Structural Journal, 111*(2), 363–374. https://doi.org/10.14359/51686535

Hallgren, M. (1996). Punching shear capacity of reinforced high strength concrete slabs. *KTH Royal Institute of Technology* .

Hegger, J., Ricker, M., & Sherif, A. G. (2009). Punching strength of reinforced concrete footings. *ACI Structural Journal, 106*(5), 706–716.

Jang, J. I., & Kang, S. M. (2021). Punching shear behavior of shear reinforced slab-column connection with varying flexural reinforcement. *International Journal of Concrete Structures and Materials, 13*(1), 29. https://doi.org/10.1186/s40069-019-0341-4

Jeong, H., Choi, S. H., Han, S. J., Kim, J. H., Lee, S. H., & Kim, K. S. (2021). Explainable models to estimate the effective compressive strength of slab-column joints using genetic programming. *Structural Concrete, 22*(6), 3491–3509. https://doi.org/10.1002/suco.202100149

Jin, Y., Yi, W. J., & Hu, L. (2017). Experimental study of performance of reinforced concrete slab-column connection with punching shear keys. *Industrial Construction, 47*(4), 60–65. https://doi.org/10.13204/j.gyjz201704014

Jin, Y., Yi, W., Hu, L., & Ma, K. (2019). Experimental analysis on mechanical performances of reinforced concrete two-way slab with studs. *Journal of Civil and Environmental Engineering, 41*(3), 77–84. https://doi.org/10.11835/j.issn.2096-6717.2019.052

Jones, D. R., Schonlau, M., & Welch, W. J. (1998). Efficient global optimization of expensive black-box functions. *Journal of Global Optimization, 13*(4), 455–492. https://doi.org/10.1023/A:1008306431147

Ju, H. J., Lee, D. K., Park, M. K., & Memon, S. A. (2021a). Punching shear strength model for reinforced concrete flat plate slab-column connection without shear reinforcement. *Journal of Structural Engineering, 147*(3), 04020358. https://doi.org/10.1061/(ASCE)ST.1943-541X.0002939

Ju, M., Ju, J. J. W., & Sim, J. (2021b). A new formula of punching shear strength for fiber reinforced polymer (FRP) or steel reinforced two-way concrete slabs. *Composite Structures, 259*, 113471. https://doi.org/10.1016/j.compstruct.2020.113471

Jumaa, G. B., & Yousif, A. R. (2018). Punching shear capacity of FRP-reinforced concrete beams without stirrups by artificial neural networks, gene expression programming, and regression analysis. *Advanced Civil Engineering*. https://doi.org/10.1155/2018/5157824

Kang, S. M., Na, S. J., Hwang, H. J., & Kim, S. I. (2021). Punching shear strength improved by upward panel in reinforced concrete transfer slabs. *Journal of Building Engineering, 46*, 103753. https://doi.org/10.1016/j.jobe.2021.103753

Khan, M. I., Abbas, Y. M., Fares, G., & Alqahtani, F. K. (2023). Strength prediction and optimization for ultrahigh-performance concrete with low-carbon cementitious materials-XG boost model and experimental validation. *Construction and Building Materials, 387*, 131606. https://doi.org/10.1016/j.conbuildmat.2023.131606

Kim, K., Kim, W., Seo, J., Jeong, Y., Lee, M., & Lee, J. (2022). Prediction of concrete fragments amount and travel distance under impact loading using deep neural network and gradient boosting method. *Materials, 15*(3), 1045. https://doi.org/10.3390/ma15031045

Koo, S., Choi, J., & Kim, C. (2020). Predicting long-term deformation of soundproofing resilient materials subjected to compressive loading: Machine learning approach. *Materials, 13*(18), 4133. https://doi.org/10.3390/ma13184133

Lewinski, P. M., & Wiech, P. P. (2020). Finite element model and test results for punching shear failure of RC slabs. *Archives of Civil and Mechanical Engineering, 20*(2), 36. https://doi.org/10.1007/s43452-020-00037-x

Li, K., Pan, L., & Wang, Y. F. (2023). Random forest-based modelling of parameters of fractional derivative concrete creep model with Bayesian optimization. *Materials and Structures, 55*(8), 215. https://doi.org/10.1617/s11527-022-02054-z

Liang, M. F., Chang, Z., Wan, Z., Gan, Y. D., Schlangen, E., & Savija, B. (2021). Interpretable Ensemble-Machine-Learning models for predicting creep behavior of concrete. *Cement and Concrete Composites, 125*, 104295. https://doi.org/10.1016/j.cemconcomp.2021.104295

Liang, S. X., Shen, Y. X., & Ren, X. D. (2022). Comparative study of influential factors for punching shear resistance/failure of RC slab-column joints using machine-learning models. *Structures, 45*, 1333–1349. https://doi.org/10.1016/j.istruc.2022.09.110

Lima, H., Palhares, R., de Melo, G. S., & Oliveira, M. (2020). Experimental analysis of punching shear in flat slabs with variation in the anchorage of shear reinforcement. *Structural Concrete, 22*(2), 1165–1182. https://doi.org/10.1002/suco.202000158

Liu, K. H., Zheng, J. K., Pacheco, T. F., & Zhao, X. Y. (2022). Innovative modeling framework of chloride resistance of recycled aggregate concrete using ensemble-machine-learning methods. *Construction and Building Materials, 337*, 127613. https://doi.org/10.1016/j.conbuildmat.2022.127613

Lovrovich, J. S., & Mclean, D. I. (1990). Punching shear behavior of slabs with varing apan-depth ratios. *ACI Structural Journal, 87*(5), 507–511.

Lundberg, S.M., & Lee, S.I. (2017). A unified approach to interpreting model predictions. in: 31st Conference on Neural Information Processing Systems, Long Beach, CA

Ma, G., Qin, C. X., Hwang, H. J., & Zhou, Z. Z. (2023). Data-driven models for predicting tensile load capacity and failure mode of grouted splice sleeve connection. *Engineering Structures, 289*, 116236. https://doi.org/10.1016/j.engstruct.2023.116236

Mangalathu, S., Hwang, S. H., & Jeon, J. S. (2020). Failure mode and effects analysis of RC members based on machine-learning-based SHapley Additive exPlanations (SHAP) approach. *Engineering Structures, 219*, 110927. https://doi.org/10.1016/j.engstruct.2020.110927

Mangalathu, S., Shin, H., Choi, E., & Jeon, J. S. (2021). Explainable machine learning models for punching shear strength estimation of flat slabs without transverse reinforcement. *Journal of Building Engineering, 39*, 102300. https://doi.org/10.1016/j.jobe.2021.102300

Muttoni, A., & Ruiz, M. F. (2019). From experimental evidence to mechanical modeling and design expressions: The critical shear crack theory for shear design. *Structural Concrete, 20*(4), 1464–1480. https://doi.org/10.1002/suco.201900193

Muttoni, A., Ruiz, M. F., & Simoes, J. T. (2017). The theoretical principles of the critical shear crack theory for punching shear failures and derivation of consistent closed-form design expressions. *Structural Concrete, 19*(1), 174–190. https://doi.org/10.1002/suco.201700088

Ngo, T. T., Le, Q. H., Nguyen, D. L., Kim, D. J., & Tran, N. T. (2023). Experiments and prediction of direct tensile resistance of strain-hardening steel-fibre-reinforced concrete. *Magazine of Concrete Research*. https://doi.org/10.1680/jmacr.22.00060

Nguyen, H., Vu, T., Vo, T. P., & Thai, H. T. (2021). Efficient machine learning models for prediction of concrete strengths. *Construction and Building Materials, 266*(B), 120950. https://doi.org/10.1016/j.conbuildmat.2020.120950

Pan, P. F., Du, J. S., Ma, H. X., & Sun, D. (2022). Data driven strength and strain enhancement model for FRP confined concrete using Bayesian optimization. *Structures, 41*, 1345–1358. https://doi.org/10.1016/j.istruc.2022.05.093

Pang, B., Wang, F. L., Yang, J., Nyunn, S., & Azim, I. (2021). Performance of slabs in reinforced concrete structures to resist progressive collapse. *Structures, 33*, 4843–4856. https://doi.org/10.1016/j.istruc.2021.04.092

Rankin, G. I. B., & Long, A. E. (2019). Punching strength of conventional slab-column specimens. *Engineering Structures, 178*, 37–54. https://doi.org/10.1016/j.engstruct.2018.10.014

Ribeiro, M.T., Singh, S., & Guestrin, C. (2016). Why should I trust you: Explaining the predictions of any classifier. In: Proceedings of the 22nd ACM SIGKDD international conference on knowledge discovery and data mining

Rojek, R., & Keller, T. (2007). Durchstanzversuche mit bewehrung mit hochfestem verbund, innovativetraganalysen und bemessungsansätze. *Stahlbetonbau, 102*, 548–556. https://doi.org/10.1002/best.200700560

Ruiz, M. F., & Muttoni, A. (2009). Applications of critical shear crack theory to punching of reinforced concrete slabs with transverse reinforcement. *ACI Structural Journal, 106*(4), 485–494.

Ruiz, M. F., Muttoni, A., & Sagaseta, J. (2015). Shear strength of concrete members without transverse reinforcement: A mechanical approach to consistently account for size and strain effects. *Engineering Structures, 99*, 360–372. https://doi.org/10.1016/j.engstruct.2015.05.007

Sabzekar, M., & Hasheminejad, S. M. H. (2021). Robust regression using support vector regressions. *Chaos Solitons and Fractals, 144*, 110738. https://doi.org/10.1016/j.chaos.2021.110738

Said, M., Mahoud, A. A., & Salah, A. (2020). Performance of reinforced concrete slabs under punching loads. *Materials and Structures, 53*(4), 68. https://doi.org/10.1617/s11527-020-01509-5

Scholkopf, B., Smola, A. J., Williamson, R. C., & Bartlett, P. L. (2021). New support vector algorithms. *Neural Computation, 12*(5), 1207–1245. https://doi.org/10.1162/089976600300015565

Schonlau, M., & Zou, R. Y. (2021). The random forest algorithm for statistical learning. *Stata Journal, 20*(1), 3–29. https://doi.org/10.1177/1536867X20909688

Seeger, M. (2004). Gaussian processes for machine learning. *International Journal of Neural Systems, 14*(2), 69–106. https://doi.org/10.1142/S0129065704001899

Shatarat, N., & Salman, D. (2022). Investigation of punching shear behavior of flat slabs with different types and arrangements of shear reinforcement. *Case Studies in Construction Materials, 16*, e01028. https://doi.org/10.1016/j.cscm.2022.e01028

Shen, L. L., Shen, Y. X., & Liang, S. X. (2022b). Reliability analysis of RC slab-column joints under punching shear load using a machine learning-based surrogate model. *Buildings, 12*(10), 1750. https://doi.org/10.3390/buildings12101750

Shen, Y. X., Sun, J. H., & Liang, S. X. (2022c). Interpretable machine learning models for punching shear strength estimation of FRP reinforced concrete slabs. *Crystal, 12*(2), 259. https://doi.org/10.3390/cryst12020259

Shen, Y. X., Wu, L. F., & Liang, S. X. (2022a). Explainable machine learning-based model for failure mode identification of RC flat slabs without transverse reinforcement. *Engineering Failure Analysis, 141*, 106647. https://doi.org/10.1016/j.engfailanal.2022.106647

Shrikumar, A., Greenside, P., Shcherbina, A., & Kundaje, A. (2016). Not just a black box: Learning important features through propagating activation differences. proceedings of the 33rd International Conference on Machine Learning, New York, USA

Silva, J., Francisco, E. S., & Gomes, W. J. S. (2023). Machine learning models to predict the punching shear strength of reinforced concrete flat slabs. *Revista IBRACON De Estruturas e Materiais, 16*(4), e16405. https://doi.org/10.1590/s1983-41952023000400005

Simoes, J. T., Ruiz, M. F., & Muttoni, A. (2018). Validation of the critical shear crack theory for punching of slabs without transverse reinforcement by means of a refined mechanical model. *Structural Concrete, 19*(1), 191–216. https://doi.org/10.1002/suco.201700280

Stein, T., Ghali, A., & Dilger, W. (2007). Distinction between punching and flexural failure modes of flat plates. *ACI Structural Journal, 104*(3), 357–365.

Su, M., Zhong, Q. Y., Peng, H., & Li, S. F. (2021). Selected machine learning approaches for predicting the interfacial bond strength between FRPs and concrete. *Construction and Building Materials, 270*, 121456. https://doi.org/10.1016/j.conbuildmat.2020.121456

Taffese, W. Z., & Espinosa-Leal, L. (2022). Prediction of chloride resistance level of concrete using machine learning for durability and service life assessment of building structures. *Journal of Building Engineering, 60*, 105146. https://doi.org/10.1016/j.jobe.2022.105146

Tian, Y., Jirsa, J. O., & Bayrak, O. (2009). Strength evaluation of interior slab-column connections. *ACI Structural Journal, 105*(6), 692–700.

Todorov, B., & Billah, A. M. (2022). Machine learning driven seismic performance limit state identification for performance-based seismic design of bridge piers. *Engineering Structures, 255*, 113919. https://doi.org/10.1016/j.engstruct.2022.113919

Tran, V., Dang, V. Q., & Ho, L. S. (2022). Evaluating compressive strength of concrete made with recycled concrete aggregates using machine learning approach. *Construction and Building Materials, 323*, 126578. https://doi.org/10.1016/j.conbuildmat.2022.126578

Truong, G. T., & Choi, K. K. (2018). Punching strength of concrete footings based on the compression zone failure mechanism. *Structures and Buildings*. https://doi.org/10.1680/jstbu.17.00135

Truong, G. T., Choi, K. K., & Kim, C. S. (2022a). Implementation of boosting algorithms for prediction of punching shear strength of RC column footings. *Structures, 46*, 521–538. https://doi.org/10.1016/j.istruc.2022.10.085

Truong, G. T., Hwang, H. J., & Kim, C. S. (2022b). Assessment of punching shear strength of FRP-RC slab-column connections using machine learning algorithms. *Engineering Structures, 255*, 113898. https://doi.org/10.1016/j.engstruct.2022.113898

Walker, R. (2014). Critical review of EC2 regarding punching and improving the design approach. Doctor's thesis, Leopold-Franzens-University Innsbruck

Wu, L. F., Huang, T. C., Tong, Y. L., & Liang, S. X. (2022). A Modified compression field theory based analytical model of RC slab-column joint without punching shear reinforcement. *Buildings, 12*(2), 226. https://doi.org/10.3390/buildings12020226

Zhang, W. G., Wu, C. Z., Zhong, H. Y., Li, Y. Q., & Wang, L. (2021). Prediction of undrained shear strength using extreme gradient boosting and random forest based on Bayesian optimization. *Geoscience Frontiers, 12*(1), 469–477. https://doi.org/10.1016/j.gsf.2020.03.007

Publisher's Note

Hua-Jun Yan First Author and corresponding Author, Ph.D. Candidate, School of Civil Engineering, Beijing Jiaotong University, Beijing, 100044, China

Nan Xie Second Author, Professor, School of Civil Engineering, Beijing Jiaotong University, Beijing, 100044, China.